ELSEVIER

Biophysical Chemistry 94 (2001) 245–256

Biophysical Chemistry

www.elsevier.com/locate/bpc

Phase memory relaxation times of spin labels in human carbonic anhydrase II: pulsed EPR to determine spin label location

M. Huber[a,*], M. Lindgren[b,1], P. Hammarström[c,2], L.-G. Mårtensson[c], U. Carlsson[c], G.R. Eaton[d], S.S. Eaton[d]

[a]*Department of Molecular Physics, Leiden University, P.O. Box 9504, 2300 RA Leiden, The Netherlands*
[b]*IFM-Department of Chemical Physics, Linköping University, 58 183 Linköping, Sweden*
[c]*IFM-Department of Biochemistry, Linköping University, 58 183 Linköping, Sweden*
[d]*Department of Chemistry and Biochemistry, University of Denver, Denver, Co 80208-2436, USA*

Received 17 July 2001; received in revised form 10 October 2001; accepted 12 October 2001

Abstract

Phase memory relaxation times (T_M or T_2) of spin labels in human carbonic anhydrase II (HCA II) are reported. Spin labels (*N*-(1-oxyl-2,2,5,5-tetramethyl-3-pyrrolidinyl)iodoacetamide, IPSL) were introduced at cysteines, by site-directed mutagenesis at seven different positions in the protein. By two pulse electron paramagnetic resonance (EPR), electron spin echo decays at 45 K are measured and fitted by stretched exponentials, resulting in relaxation parameters T_M and x. T_M values of seven positions are between 1.6 μs for the most buried residue (L79C) and 4.7 μs for a residue at the protein surface (W245C). In deuteriated buffer, longer T_M are found for all but the most buried residues (L79C and W97C), and electron spin echo envelop modulation (ESEEM) of deuterium nuclei is observed. Different deuterium ESEEM patterns for W95C and W16C (surface residue) indicate differences in the local water concentration, or accessibility, of the spin label by deuterium. We propose T_M as a parameter to determine the spin label location in proteins. Furthermore, these systems are interesting for studying the pertaining relaxation mechanism.

Keywords: Spin label EPR; Relaxation; Human Carbonic Anhydrase II; T_2

1. Introduction

Spin labeling has proven useful for structural investigations of proteins. New impulses for using spin label Electron Paramagnetic Resonance (EPR) techniques come from the technical and methodological development in EPR. Here we focus on pulsed EPR. Specifically, the phase memory relaxation times (T_M or T_2) of the electron spins are investigated in order to characterize the location of a spin label in proteins of unknown structures. The protein investigated is human carbonic anhydrase II (HCA II), a largely sheet protein (see Fig. 1). The structure of HCA II is known from X-ray crystallography [1], making it

* Corresponding author. Tel: +31-71-527-5560; fax: +31-71-527-5819.
E-mail address: mhuber@molphys.leidenuniv.nl (M. Huber).
[1] Present address: Defence Research Establishment, Institute of Sensor Technology, Department of Laser systems (FOA32) SE-581 11 Linköping, Sweden.
[2] Present address: The Scripps Research Insitiute, The Skaggs Institute for Chemical Biology, 10550 North Torrey Pines Road MB 12, La Jolla, California 92037 USA.

0301-4622/01/$ - see front matter
PII: S0301-4622(01)00239-3

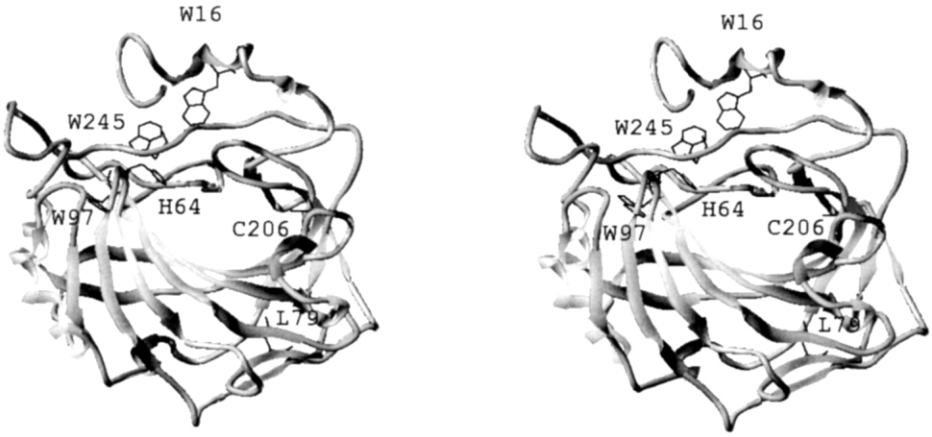

Fig. 1. Stereo view of human carbonic anhydrase (HCA II) with positions W97C, L79C, C206, F176C, W245C, W16C and H64C used for spin labeling indicated.

a suitable model to study the influence of the structure on the relaxation parameters. Spin labeling by site directed mutagenesis, as introduced by Millhauser [2] and Hubbell and Altenbach [3], also termed site directed spin labeling (SDSL), is used to incorporate the spin labels at the desired positions. In HCA II, labeling sites are well-established, and different labeling methods have been employed to characterize a large number of protein positions ranging from buried to surface exposed residues. In [4,5] the results of different labeling techniques are compared, including the accessibility and the polarity of sites by fluorescence techniques. Information about the spin label mobility by continuous wave (cw) EPR is given in [5–8].

Prior investigations of spin labeled HCA II [9] have shown, that T_M varies with the spin label position and that the electron spin echo decays can be described by a stretched exponential. A model was proposed to interpret the dependence of T_M on the spin label environment. More recent studies of nitroxide and other radicals in different solvent systems give more detailed information about the factors determining electron spin echo decays [10]. T_M depends on the proton concentration, and the concentration and mobility of methyl groups in the medium surrounding the spin label. In general, increasing proton concentration was found to decrease T_M. Freely rotating methyl groups enhance relaxation, resulting in even smaller T_M values.

In [9] five positions in HCA II were compared (W97C, W123C, S56C, C206, F176C). The goal of the present study is to examine a wider range of probe locations than in [9] and to interpret the data with respect to the findings in [10]. In the present study, seven positions were investigated (see Fig. 1), including three previously studied sites (W97C, C206 and F176C) plus four additional sites (L79C, W245C, W16C and H64C). Overlapping positions compared to [9] were chosen to test reproducibility and the additional positions give a more complete sample of environments than previously available. In addition, a more systematic investigation of the effect of exchanging the buffer with deuteriated buffer is performed, since in [9] only two sites (W123C and F176C) were investigated in deuteriated buffer. The systematic investigation of the spin labeled proteins in deuteriated buffer, which had not been performed in the previous study [9], is important for the mechanistic interpretation of T_M and x values. It is also of diagnostic value, to better distinguish spin label positions close to the protein surface. Three methods of analyzing spin echo decays to determine T_M and x in the presence of deuterium spin echo modulation are evaluated.

2. Materials and methods

Mutants were made and spin labeling using *N*-(1-oxyl-2,2,5,5-tetramethyl-3-pyrrolidinyl)iodoacetamide (IPSL) was performed as described in [11]. HCA II contains a native cysteine, (C206), which was spin labeled in the sample referred to as C206. In all mutants, C206 is replaced by serine (C206S) in addition to the mutation introducing the cysteine at the desired position. Glycerol was added in a 1:1 (v/v) ratio before freezing the samples. The final sample concentration of the different mutants was between 0.02 and 0.3 mM. Samples were degassed by three freeze-pump-thaw cycles on the vacuum line and sealed under vacuum. D_2O exchange was performed by diluting samples into ^{2}H-buffer and concentrating, again, three times. Before freezing, these samples were diluted in a 1:1 (v/v) ratio with glycerol-d_8 (^{2}H-buffer) and degassed as described above.

Measurements were performed on a Bruker Elexsys E580 spectrometer using an Oxford ER 935 cryostat. Two pulse echo decays were measured with the $\pi/2$-τ-π pulse sequence with pulse lengths of 16 ($\pi/2$) and 32 ns (π) or 80 ($\pi/2$) and 160 ns (π). For several mutants both pulse lengths were tried and did not result in differences in the decay times. The longer pulses were found to be preferable, because the limited excitation bandwidth reduces unwanted electron spin echo envelope modulation due to protons. Echo decay curves and parameters reported in the following refer to pulse parameters of 80–160 ns. Under these conditions, dead times were estimated to be 440 ns. As discussed [9], instantaneous diffusion can decrease T_M. To test for spin diffusion, the flip angle was varied by changing the microwave power of the pulses. For several cases, no dependence of T_M on pulse turning angle was found, which indicated that the effects of spin diffusion were negligible for these samples. Therefore, pulse powers were adjusted to give maximum echo intensity, i.e. flip angles of 90 and 180°, respectively. Measuring the temperature dependence of decay times within the range of 30–70 K for several of the mutants revealed no significant differences. Thus, decay times are reported for 45 K. In all measurements the static magnetic field was set to the maximum of the spin label EPR signal, i.e. the central line of the frozen solution EPR spectrum.

2.1. Fitting data to obtain T_M

In analogy to a previous study [9], decay curves are fitted to a stretched exponential function of the form:

$$Y(\tau) = Y(0)\exp[-(2\tau/T_M)^x] \quad (1)$$

where τ is the time between the two pulses, T_M the phase memory time, x the exponent and $Y(0)$ the echo intensity at $\tau = 0$. Fitting was performed by a least squares fitting procedure using the Marquardt algorithm in the Matlab program (The MathWorks Inc.). This approach was not feasible for samples in ^{2}H-buffer because deuterium electron spin echo envelop modulation (ESEEM) dominates the electron spin echo decay curve. Therefore, three approaches were examined for the analysis of the samples in ^{2}H-buffer.

Method 1: the parameters of the stretched exponential, i.e. the decay time T_M and the exponent x, were adjusted manually to match the curve to the maxima of the experimental decay.

Method 2: the following procedure was used to eliminate the modulation from the experimental decay curve, which was then fitted as described above for the samples in the ^{1}H-buffer system. The experimental two pulse echo data (Y_{exp}) is the product of the modulation (Y_{mod}) and the decay (Y_{decay}) functions [12]:

$$Y_{exp} = Y_{decay} Y_{mod} \quad (2)$$

The modulation (Y_{mod}) reflects the hyperfine interaction of the electron and the deuterium nuclear spins, and was simulated as described in Section 2.2, resulting in a simulated modulation curve Y_{mods}.

$$\frac{Y_{exp}}{Y_{mods}} = Y_{decay} \quad (3)$$

Y_{mods} is then used to eliminate the modulation and a decay curve (Y_{decay}) is obtained, which is largely devoid of the modulation [Eq. (3)]. The

decay Y_{decay} was then fitted with the least square fitting procedure described above.

Method 3: The first part of the electron spin echo decay curve was removed resulting in a curve starting at 1.5 μs from $\tau = 0$, i.e. 1.5 μs including the experimental dead time. This procedure removes the first few periods of the modulation. The remainder of the curve can then be analyzed by the least squares fitting procedure described above because the remaining modulation periods are relatively shallow compared with the echo amplitude. For the mutants with relaxation times on the order of the truncation value of 1.5 μs (L79C and W97C) this method cannot be applied. T_M and x values obtained by method 3 depend on the starting time of the fitting, thus the curves for all samples had to be truncated to the same starting value.

2.2. Deuterium modulation

The modulation Y_{mod} was simulated using a program developed by Lund. The program is based on an extension of the methods described by Dikanov and Tsvetkov [13]. It allows for G-tensor anisotropy and inclusion of non-collinear hyperfine tensors and the quadrupolar interaction of nuclei. The treatment of hyperfine and quadrupolar interactions and powder averaging is done according to [14,15], the program is discussed in [16]. To analyze the modulation the echo decay (Y_{decay}) was eliminated from the experimental curve (Y_{exp}) using an exponential decay curve (Y_{decexp}):

$$\frac{Y_{exp}}{Y_{decexp}} = Y_{mod} \quad (4)$$

The parameters of the simulation, i.e. the number of nuclei and their hyperfine interaction parameters, were varied as to obtain the best fit to the experimental curve. The main criterion for the quality of the fit was the relative amplitude of successive modulation periods in experimental and simulated curve, respectively, as the absolute amplitude of the modulation curve at any point depends on the choice of Y_{decexp}. The simulation of Y_{mod} yields hyperfine parameters of the deuterium nuclei surrounding the spin label (see Section 3). The error of T_M in ^{1}H-buffer samples as estimated from fits to different experimental curves for one sample is $T_M \pm 0.2$ μs and $x \pm 0.2$. This is also the minimum error for samples in ^{2}H-buffer. For these samples, errors depend on the fit method and deviations between the fit parameters for the different methods of analysis are discussed below.

2.3. Position of spin label and solvent accessibility

To determine the number of methyl groups in the vicinity of the unpaired electron, the position of the N–O group of the spin label is needed. From the X-ray structure of HCA II [1] the position of the native residue is known. However, the conformation of the cysteines introduced by mutagenesis and of the attached spin label is not known. To obtain an estimate of the local environment, the position of the β carbon atom of the native amino acid residue was used to represent the spin label location. Surface accessibility is a parameter that reflects the location of an amino acid residue in a protein. Surface accessibility of the native side chain was calculated using a probe radius of 1.4 Å as described by Connolly [17]. Fractional accessibility surface area was calculated as the ratio of the absolute area of each amino acid divided by the area of the exposed area of each amino acid situated in an exposed tripeptide, Ala-X-Ala, according to Lee and Richards [18]. For HCA II accessibility values for most of the residues of the present study were reported in [19].

3. Results

Fig. 2 shows echo decay curves measured for mutants W97 and F176, which demonstrate the differences in the length and the shape of the decays that are attributed to the location of the spin label in the protein. The decays are non-exponential and were fitted to a stretched exponential function [Eq. (1)] [9]. The resulting fit parameters T_M, the phase memory times and x the exponents are listed in Table 1. In Table 1 entries are ordered from buried to surface-exposed residues from left to right (see Section 4). The values exhibit a systematic increase of T_M and to some degree also of x with increasing solvent exposure.

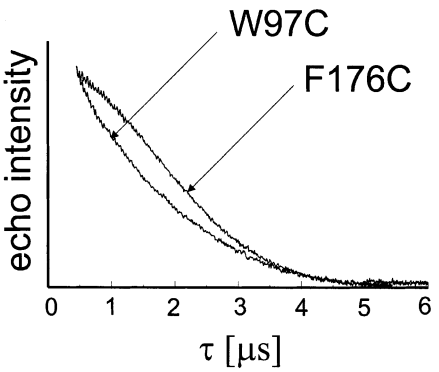

Fig. 2. Electron spin echo decay curves for HCA II spin labeled at position W97C and F176C. T= 45 K, pulse lengths: 80 ns and 160 ns. τ: time between first and second microwave pulse. The initial time includes a dead time of 440 ns.

mixtures (see Section 2). Fig. 3 shows the resulting decay curves for W97C and W16C. Pronounced ESEEM patterns are observed, whose frequencies correspond to those expected for deuterium. To extract the decay parameters in the presence of the modulation, three methods were examined (see Section 2). The values obtained by all three methods are compared in Table 2. The shorter T_M times in mutants L79C and W97C made it impossible to apply methods 2 or 3 to L79C or to apply method 3 to W97C. The relatively large differences in T_M and x values obtained by the three methods (Table 2) show that, due to the modulation, T_M and x cannot be determined as accurately in the ^{2}H-buffer as in the ^{1}H-buffer. The uncertainty in x is particularly large because the impact of x is

Table 1
T_M of spin-labeled human carbonic anhydrase II and comparison with information concerning probe location

Residue		L79C	W97C	C206	F176C	W245C	W16C	H64C
Location		buried	buried	buried	at/near surface	surface/intermediate	surface	
Probe mobility[a]		rigid	rigid	rigid	mobile	rigid/mobile	mobile	rigid/mobile
Solvent accessible surface area [Å^2][b]		0.00	0.00	0.01	0.09	0.22	0.01[c]	0.37
Number[d] of CH_3		24	15	11	13	6	7	2
		Group 1		Group 2		Group 3		
H_2O/glycerol	T_M [μs]	1.6	2.7[e]	3.8[f]	3.7[g]	4.7	4.3	4.5
	x	1.2	1.3[e]	2.0[f]	1.8[g]	2.4	2.1	2.0
D_2O/glycerol-d_8	T_M [μs][h]	1.4[i]	2.7	6.0	5.8[g]	9.0	12.6	n.d.[j]
	x[h]	1.0	0.9	1.0	0.9[g]	1.6	1.3	n.d.
$\Delta(1/T_M)$[μs^{-1}]		≈0	≈0	0.10	0.10	0.10	0.15	

[a] From mobility descriptors reported in [5–8], H64C: Lindgren, personal communication.
[b] Fractional surface accessibility from [19], and see Section 2.
[c] From labeling and reactivity: W16 is buried, but labels attached to this position are flexible [7].
[d] Number of methyl groups in sphere between 5 and 10 Å (see Table 3).
[e] Data reported for W97C in [9] were obtained with shorter pulses that excited proton modulation. Values obtained by data analysis method 1 were T_M=2.0 μs, x=1.0. Reanalysis of the data for W97C reported in [9], using method 3 give T_M=2.4 μs, x=1.2, which is in better agreement with the values obtained here with longer pulse lengths.
[f] Values reported for C206 in [9] in ^{1}H-buffer: T_M=4.1 μs, x=2.0.
[g] Values reported for F176C in [9] in ^{1}H-buffer: T_M=4.1 μs x=1.9; in ^{2}H-buffer T_M=5.5 μs, x=1.0, when analyzed by method 1. Analysis by method 3 gives T_M=8.0 μs, x=1.3.
[h] Parameters from least squares fit of decay with modulations removed (method 2, see Section 2.1), unless otherwise stated.
[i] From method 1 (see Section 2.1).
[j] n.d.: not determined.

To determine the contribution of protons in the buffer/glycerol mixture to T_M, spin labeled proteins were investigated in ^{2}H-buffer/glycerol-d_8 greatest in the early portion of the decay curve, where the modulation is deepest. As described in Section 4, method 2, in principle, should be the

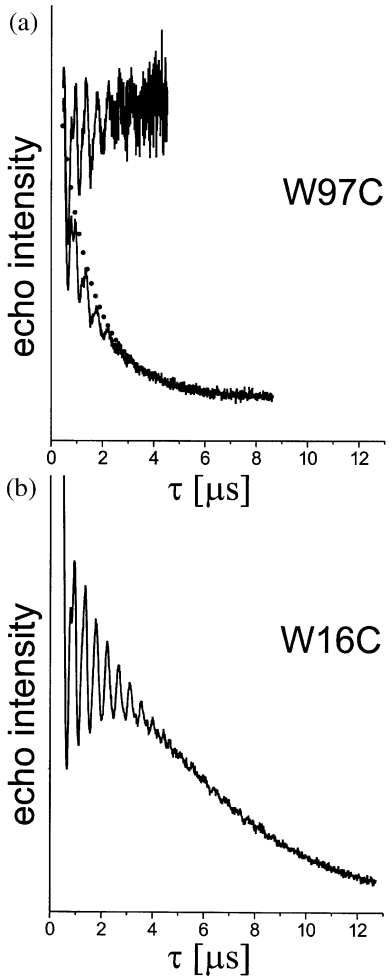

Fig. 3. Electron spin echo decay curves for HCA II spin labeled at position W97C (a) and position W16C (b) in glycerol-d_8/D_2O. Note the deep modulation due to deuterium. Upper trace in (a) modulation extracted (Y_{mod}, see text), dotted line: simulated decay, method 1, see text.

most reliable, so values obtained by this method are given in the summary Table 1, except for L79C, where method 1 was used.

For all of the mutants, except for L79C and W97C, modulation frequencies and depths are similar. Thus, the modulation is expected to result in similar systematic errors in all the samples. Analogous to the results in ^{1}H-buffer, the T_M values of samples in ^{2}H-buffer show a systematic variation of the decay parameters with respect to the position of the spin label. For buried sites L79C and W97C, T_M values are unchanged by deuteriation, within experimental uncertainty. For sites C206, F176 and W245C, deuteriation of the buffer causes a substantial increase in T_M. The largest impact was observed for W16C, which is judged to be at the surface.

3.1. Deuterium modulation

The ESEEM patterns for L79C and W97C differ from those of the remaining mutants (Fig. 4). For L79C the echo decay is too fast to analyze the modulation, so W97C was selected as an example of modulation at a buried site. The modulation for W16C was selected as an example of an exposed site (see Table 1 and Section 4). By dividing the experimental curve Y_{exp} by Y_{decexp}, a curve dominated by the modulation (Y_{mod}) was obtained [Eq. (4)]. For the simulations [16], the G- tensor was taken to be isotropic and hyperfine (hf) parameters of the deuterium were varied until the best agreement of the experimental (Y_{mod}) and simulated (Y_{mods}) modulation was obtained. The quadrupole interaction was not included. The hf interaction is described by the hyperfine tensor $\underline{A} = \underline{1}\, A_{iso} + \underline{A}_{dip}$. The simulation parameters are essentially A_{iso} and A_{dip}, as the principal values of $\underline{A}_{dip}$ are $2A_{dip}$, $-A_{dip}$ and $-A_{dip}$, where A_{dip} is the perpendicular eigenvalue of the hyperfine tensor (for background, see for example [20]). Hyperfine tensors of multiple nuclei were taken to be collinear. For W97C, satisfactory agreement of simulations and experiment was obtained using 4 nuclei of $I=1$, with $A_{iso}=0.8$ MHz, and a dipolar contribution of

Table 2
Comparison of fitting methods for determining T_M and x in spin-labeled human carbonic anhydrase II in glycerol-d_8/D_2O buffer

	Method 1		Method 2		Method 3	
	T_M [μs]	x	T_M [μs]	x	T_M [μs]	x
L79C	1.4	1.0				
W97C	2.4	0.9	2.7	0.9		
C206	4.2	1.0	6.0	1.0	7.4	1.2
F176C	4.3	0.9	5.8	0.9	8.8	1.5
W245C	6.0	1.0	9.0	1.6	9.6	1.8
W16C	9.1	0.9	12.6	1.3	15.4	1.6

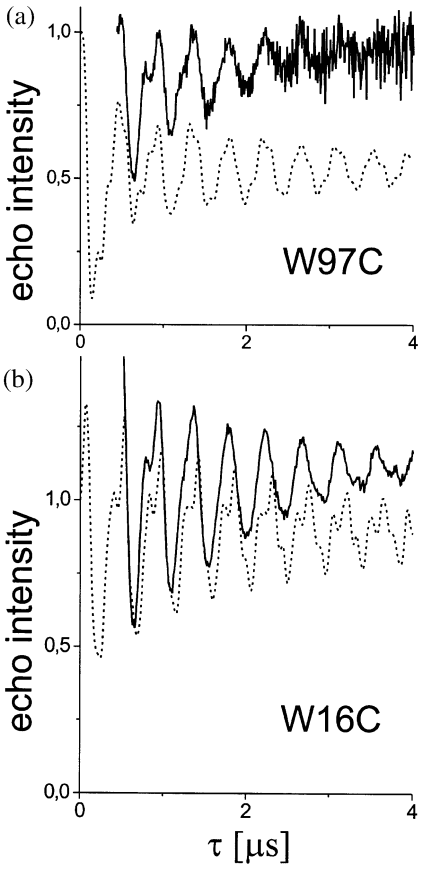

Fig. 4. Electron spin echo decay modulation of HCA II spin labeled at position W97C (a) and W16C (b) in glycerol-d_8/D_2O. Solid line: experimental, broken line: simulation. Parameters used for the simulation: isotropic G-tensor and 4 nuclei of $I=1$, with $A_{iso}=0.8$ MHz and a dipolar contribution $A_{dip}=1$ MHz (a). For W16C (b), Set 1: 4 nuclei of $I=1$, $A_{iso}=1.3$ MHz, $A_{dip}=1.4$ MHz; set 2: 6 nuclei of $I=1$, $A_{iso}=0$ MHz, $A_{dip}=0.2$ MHz.

$A_{dip}=1$ MHz (Fig. 4a). In the case of W16C, two sets of nuclei with different hf parameters gave better agreement than a single set. Set 1 consisted of 4 nuclei of $I=1$, with $A_{iso}=1.3$ MHz and a dipolar contribution $A_{dip}=1.4$ MHz, and the second set of 6 nuclei of $I=1$, with a purely dipolar contribution of $A_{dip}=0.2$ MHz ($A_{iso}=0$ MHz) (Fig. 4b). The agreement of experimental and simulated modulation patterns is acceptable, but given the large number of parameters entering the simulation, the fit is unlikely to be unique. The modulation for C206, F176C and W245C is similar in shape and intensity to that of W16C, suggesting that the patterns are dominated by similar hyperfine interactions. The simulated modulation curves were used as Y_{mods} to extract Y_{dec} [Eq. (3)] for data analysis method 2.

4. Discussion

The electron spin echo decay parameters of spin labels introduced at seven positions throughout the protein are presented. Comparison with the previous study [9] shows that the T_M and x parameters of C206 (in ^{1}H-buffer) and W97C, F176C (in ^{1}H- and ^{2}H-buffer), see Table 1, agree, within experimental error, with those determined earlier [9], indicating that these parameters are well reproducible with respect to different batches of protein preparation and different spectrometer configurations.

The location of the residues to which spin labels were attached is characterized by the solvent accessible area listed in Table 1. From activity and spectroscopic evidence, gross structural changes in the protein upon spin labeling have been excluded [5,7,8], nevertheless, locally, the orientation of the spin label may differ from that of the residue replaced by it. The most obvious example is W16 in HCA II. EPR of W16C shows a mobile spectrum indicating a surface exposed location, while the solvent accessible value suggests that W16 is buried [7].

4.1. Values of T_M and x

On the basis of the measured values of T_M, the mutants were divided into three groups comprising L79C and W97C with short; C206 and F176C with intermediate; and W16C, H64C and W245C with longer relaxation times. While the first group is also characterized by small values of x, the difference in x between the second and third groups is not significant.

T_M and x parameters of the group 3 locations compare well with those of the PROXYL (3-carbamoyl-2,2,5,5-tetramethylpyrrolidin-1-yloxyl) spin label in 1:1 glycerol:H_2O ($T_M=4.4$ μs, $x=2.1$) and for TEMPONE (2,2,6,6-tetramethyl-

4oxo-piperidin-1-oxyl) in solvents with proton concentrations between 110 and 120 M and no methyl groups ($T_M = 4.2-5.2$ μs, $x = 2.1-2.4$) [10], suggesting that the decay parameters of spin labels at these positions are largely determined by non-methyl protons in the protein and from the buffer/solvent mixture in which the protein is dissolved. The relative importance of contributions from protein and solvent protons was examined by replacing the ^{1}H-buffer with a glycerol-d_8/D_2O buffer system. The deuterons in the ^{2}H-buffer cause ESEEM (Fig. 3), which makes the analysis of T_M and x less straightforward than for the decays in the ^{1}H-buffer. Three different methods of analysis were used to analyze the data in ^{2}H-buffer (Table 2, Section 2).

Method 1, in which the simulated decay curve is adjusted to fit to the maxima in the echo decay curve, gave the shortest T_M values. The decay constant obtained by this method includes both the intrinsic echo decay and the damping of the modulations that occurs because of the distributions of the modulation frequencies (Fig. 4). Therefore, matching the decay to the maxima of the modulated curve results in apparent T_M values that are shorter than the value only due to the echo dephasing. In method 2, the experimental data were divided by a simulated modulation curve to give an estimated decay curve. The validity of method 2 depends critically on the quality of the simulation of the modulation, and any deviation between the simulated and experimental modulation amplitudes, in particular with respect to the amplitudes of successive periods of modulation, will affect T_M. It is particularly difficult to simulate the first few periods of the modulation because of the experimental dead time. The dead time has an impact on the ability to estimate x, because the shape of the echo decay curve at early times is more strongly dependent on x than the later portions of the curve.

In method 3, a least squares procedure was used to fit a stretched exponential to the data including the modulation. Since the amplitudes of the simulated modulation curves are approximately symmetric with respect to a constant average (see Fig. 4), this is a reasonable approximation. The drawback of method 3 is that the modulation during the initial part of the echo decay curve is so deep that the fit is dependent on the starting point. To avoid the deepest modulation periods, the initial 1.5 μs of the data were not included in the fit. The uncertainty of the shape at early time introduces substantial uncertainty in the value of x. Trends in values of T_M obtained by the three methods are similar, with the exception of positions F176C and C206. According to method 2 they agree within experimental error, whereas method 3 gives a larger T_M for F176C. The origin of this difference is not clear, but may well be an indication of uncertainties in the analysis. The values obtained by method 2 are included in Table 1 because, in principle, complete simulation should give results that are more precise than the other two methods.

For L79C and W97C (Table 1) there is no significant change in T_M upon deuteration, whereas for spin labels at other positions T_M, values in ^{2}H-buffer are longer than in ^{1}H-buffer. Contributions to echo dephasing combine approximately as the sum of the reciprocals of time constants for contributing processes [10]. The change in relaxation rate $\Delta(1/T_M) = (1/T_M \text{ in } ^1\text{H-solvent}) - (1/T_M \text{ in } ^2\text{H-solvent})$ is included in Table 1. Although uncertainties in T_M in deuteriated solvents cause uncertainties in the absolute magnitudes of the values of $\Delta(1/T_M)$, trends are likely to be reliable. Deuterons are less effective in spin echo dephasing because the magnetic moment of a deuteron is significantly smaller than that of a proton and, therefore, electron–deuteron dipolar coupling is smaller than electron–proton dipolar coupling. Thus, spin flips of neighboring deuterons have less impact on the local field experienced by the electron than flips of neighboring protons (see [8,9] and references therein). These effects extend over distances up to approximately 20 Å [10] and thus reflect the environment of the spin label over a substantially longer distance than is detected by ESEEM, which detects primarily interactions at less than approximately 5 Å. The negligible differences in echo dephasing between ^{1}H and ^{2}H solvents for L79C and W97C indicate that water/buffer nuclei play little role in the dephasing at these buried sites. By contrast, the substantial impact of solvent deuteration for the more exposed

sites indicates that solvent protons play significant roles in the dephasing at these sites. The larger value of $\Delta(1/T_M)$ for W16C than for C206, F176C and W245C indicates greater solvent exposure at W16C. Even so, the values of T_M for all of the spin-labeled proteins are substantially shorter than the approximately 100 μs observed for TEMPONE in D_2O/glycerol-d_8 (Eaton and Eaton, unpublished results), which indicates that protein protons make a substantial contribution to the dephasing for all of the spin labels. When the buffer is deuteriated, the only protons available are those of the protein. Thus, even small differences in the number and type of protons of the protein in the vicinity of the spin label and differences in distance of the probe from the surface of the protein can cause larger changes in T_M values in ^{2}H-buffer than in ^{1}H-buffer. Due to the difficulties in obtaining reliable values for the exponent x by any of the methods presented, we do not attempt to interpret differences in values of x in deuteriated solvents.

4.2. Interpretation of T_M and x

The phase memory relaxation parameters for spin labels in a series of solvents [10] give a framework for a phenomenological understanding of the molecular origin of the measured parameters characterizing the electron spin echo decay. The density of protons and the density and type of methyl groups have been identified as key parameters for electron spin echo dephasing [10]. As the density of protons increases, T_M decreases, and in solvents without methyl groups values of $x>2$ are often observed. Methyl groups, particularly those not sterically hindered, enhance the relaxation resulting in short T_M values and exponents at approximately 1.

As seen in Table 1 relaxation parameters for group 1 residues are close to the latter situation, whereas parameters for group 2 and 3 residues are similar to the former. The difference in the density of protons in the interior of proteins relative to the glycerol/H_2O mixture surrounding the protein is quite small, suggesting that the presence of methyl groups in the protein is the decisive parameter in explaining the shorter values of T_M at buried sites [9,10]. The fact that the buffer/glycerol mixture surrounding the protein contains no methyl groups and concentrations of methyl side chains are typically low near the surface is consistent with x values at approximately 2 for exposed sites.

Table 3
Number of methyl groups of amino acid residues in spheres of radius r centered on β-carbon of native residue that was replaced by cysteine

Radius [Å]	L79	W97	C206	F176	W245	W16	H64
5	2	1	4	3	0	0	1
10	26	16	15	16	6	7	3
15	53	42	38	29	29	12	26
5–10	24	15	11	13	6	7	2

To explain the differences in T_M values for interior positions, methyl groups around these residues are of interest. A list of the number of methyl groups in the vicinity of different positions of the spin label is compiled in Table 3. We compare the number of methyl groups in spheres of 5, 10 and 15 Å from the C-β atom of the amino acid residue that is replaced by the cysteine to which the spin label is attached. The number of methyl groups in the 5 Å sphere is too small to be significant. Furthermore, the distance between the C-β atom and the nitroxide group in the spin label is approximately 5 Å, so such a small sphere is not indicative of the environment of the paramagnetic center. On the other extreme, in a sphere of 15 Å the number of methyl groups is similar for all interior positions of the spin label, which is not surprising since HCA II is a relatively small protein. In the intermediate range, i.e. within a radius of 10 Å or in the shell between 5 and 10 Å, the number of methyl groups differs strongly depending on the position of the spin labeled residue. Also, from the modeling of decays based on the theory by Milov et al. [21] (Lindgren et al., to be published), methyl groups at distances larger than 10 Å do not have a strong effect on T_M. In Table 1 the number of methyl groups in the shell from 5 to 10 Å is compared with T_M and x values. For positions with a large number of methyl groups, short T_M and exponent x at approximately 1 are observed, whereas a small number of methyl groups are associated with a longer T_M and exponent x at approximately 2.

For example, the shortest T_M is observed for L79C, the residue surrounded by the largest number of methyl groups. The number of methyl groups surrounding C206 is similar to that for F176C and spin labels at these sites have similar values of T_M and x. While these relations are suggestive, the number of positions investigated is not sufficient to prove the suggested correlation. However, the qualitative conclusion, that interior positions are characterized by shorter T_M values and exponent x closer to 1 than to 2 can safely be drawn. Presently, a model is being developed to quantify the influence of the position and the motional dynamics of the protons surrounding the spin label on the T_M and x values, based on the theory by Milov et al. [21] (Lindgren et al., to be published). This will allow determination of the molecular parameters responsible for the relaxation times and should permit a more quantitative interpretation of the phase memory relaxation times.

4.3. ESEEM from deuterium nuclei in the D_2O buffer

When ^{1}H-buffer is replaced by glycerol-d_8/D_2O buffer, deuterium modulation is observed for all locations of the spin label, indicating that deuterons of the buffer approach closely enough to the spin label to have a significant hyperfine interaction. This is particularly noteworthy for the buried residues L79C and W97C, as it demonstrates that D_2O enters the protein near these buried sites. Simulations of the modulation allow estimation of the magnitude of the hyperfine interaction of the deuterium nuclei. The hyperfine parameters for the W97C and W16C mutants are given in Section 3. The isotropic component (A_{iso}) is due to electron spin density in the deuterium s-orbital that requires a close contact of the deuteron with the spin label. For W16C A_{iso} ($A_{iso}=1.3$ MHz) is larger than for W97C ($A_{iso}=0.8$ MHz) suggesting a stronger interaction of the electron spin with the deuteron in the former case. Also, for W16C, a second shell of deuterons with a smaller hfi is needed in the simulation of the modulation, which we attribute to the next nearest solvent molecules. In the case of W97C, this interaction does not seem to play a role, suggesting that the second solvent shell is too far from the spin label to give a significant contribution to the echo modulation or that fewer water molecules are present in the immediate vicinity of the label at buried sites. The absolute values of A_{iso} in these simulations are large compared to literature data for the interaction of spin labels with deuterons, where $A_{iso}=0.6-0.7$ MHz [22], $A_{iso}=0.9$ MHz, and a quadrupole parameter $Q=0.4$ [23] were reported. This difference may be due to the unrealistic geometry (co-linearity of hyperfine tensors) and the neglect of the quadrupolar interaction in the present simulations.

Future studies to quantitatively analyze the modulation and to derive a structural model of the deuterons around the spin label would require further simulations to improve on these aspects. In the present context, the primary purpose of the simulations was to obtain modulation curves that could serve as Y_{mods} in Eq. (3) and thereby permit determination of more accurate values of T_M and x in ^{2}H-buffer samples than could be obtained directly from the decay curves including the modulation.

4.4. Comparison with the results of continuous wave EPR

Finally, the results obtained by spin echo measurements are compared to traditional continuous wave (CW) EPR measurements of spin labeled samples in liquid solution at ambient temperatures, that were performed to determine the rotation correlation time through lineshape analysis. The mobility of the label reflects short-range interactions of the label with the protein. These results can be correlated to the present study since surface exposed residues are expected to have high mobility and buried residues should be immobilized [4,7]. By CW EPR it was shown that spin labels on L79C [5] and W97C have very low mobilities, and W16C and W245C [7] have intermediate to high mobilities (Table 1).

Interestingly, the liquid solution spectra of more immobilized spin labels almost invariably show the presence of multiple components, that are interpreted as populations of spin labels with different mobilities and attributed to different orientations of the spin label in the protein [24].

There is no indication of multiple components in the T_M measurements of spin labels in the same positions. Thus, either of the differences in orientation persists at low temperatures, but the corresponding orientations do not result in sufficiently different relaxation rates, or the spin labels reorient to one dominant conformation.

5. Summary and outlook

Spin labels at different protein positions show significantly different T_M and x values, which suggests that these parameters can serve as a diagnostic tool for spin label location. T_M values obtained on spin labeled proteins in ^{2}H-buffers can be useful to distinguish sites according to solvent accessability and to distinguish types of protons in the environment. For the analysis of echo decay times in ^{2}H-buffer three methods are presented. Method 2, which explicitly treats the modulation seems preferable. However, if an analysis of the modulation cannot be performed, method 3 is preferred over method 1. We propose that the parameters of electron spin echo decay curves can be used as an alternative or complementary method to liquid solution CW EPR to determine specific properties of the environment of a spin label. In the present phenomenological interpretation for these parameters, the density of methyl groups surrounding the spin label plays an important role. Theoretical models have been presented [9,10] and are under further development, to relate values of T_M and x to the proton environment of the spin label. The data reported here will be important to test those models, since, in contrast to a solvent environment, the location of protons in the protein can be obtained from the X-ray structure.

The ESEEM patterns of the spin-labeled protein immersed in a ^{2}H-buffer system are due to the hyperfine interaction of the electron spin and the deuterons. The hyperfine interaction depends on the distance of the nuclei from the spin label, and thus reflects the accessibility of the spin label to the buffer. The ESEEM data could be used to determine the water penetration into the interior of a protein.

An additional aspect to be addressed is the potential use T_M and x to characterize the locations of spin labels in proteins of unknown structure. Here, the relaxation parameters will permit residues to be identified as buried, intermediate or surface residues. In these cases, the location of methyl groups will not be known, but the above categories derive from the fact that there are no methyl groups in the buffer, leaving only methyl groups in the protein to shorten T_M. Using deuteriated buffer, a greater dispersion of T_M values for residues close to the surface can be expected and the methods to analyze the resulting decay curves are discussed in the present account. In practical terms, in contrast to CW EPR, these measurements are performed in frozen solutions or membranes, which can be an advantage for proteins with limited solubility or stability. In addition, by studying the immobilized samples, the impact of protein environment on T_M can be separated from effects of mobility on T_M.

Together with other recently developed methodological approaches to spin label EPR (see for example [25]), the use of pulsed EPR to determine T_M and x is a promising tool to obtain parameters for the location and the environment of spin labels.

Acknowledgements

M.H. thanks Prof. Anders Lund for providing a stimulating working environment and the material basis for the experiments. We thank Prof. Anders Lund for the simulation program and for helpful discussions. Dr Daniele Biglino is acknowledged for help with the simulation programs and Dr Nikolas Benetis for discussions. M.H thanks the NFR (Swedish National Research Foundation) for financial support as a visiting professor. Financial support from the Swedish Natural Science Research Council (U.C.) and the Wallenberg Foundation is gratefully acknowledged. Grant support from the National Institutes of Health Grant GM21156 and GM 59597 (G.R.E and S.S.E) is gratefully acknowledged.

References

[1] K.M. Håkansson, U. Carlsson, L.A. Svensson, A. Liljas, Structure of native and apo carbonic anhydrase II and structure of some its anion–ligand complexes, J. Mol. Biol. 227 (1992) 1192–1204.

[2] G.L. Millhauser, Selective placement of electron-spin-resonance spin labels-new structural methods for peptides and proteins, TIBS 17 (1992) 448–452.
[3] W.L. Hubbell, C. Altenbach, Site directed spin labeling of membrane proteins, Curr. Opin. Struct. Biol. 4 (1994) 566–573.
[4] M. Svensson, B.-H. Jonsson, P.O. Freskgard, B.H. Jonsson, M. Lindgren, L.-G. Mårtensson, M. Gentile, K. Borén, U. Carlsson, Mapping the folding intermediate of human carbonic-anhydrase-2. Probing substructure by chemical-reactivity and spin and fluorescence labeling of engineered cysteine residues, Biochemistry 34 (1995) 8606–8620.
[5] P. Hammarström, R. Owenius, L.-G. Mårtensson, U. Carlsson, M. Lindgren, High resolution probing of local conformational changes in proteins by the use of multiple labeling: Unfolding and aggregation of human carbonic anhydrase II monitored by spin, fluorescent and chemical reactivity probes, Biophys. J. 80 (2001) 2867–2885.
[6] M. Persson, P. Hammarström, M. Lindgren, B.H. Jonsson, M. Svensson, U. Carlsson, EPR mapping of interactions between spin-labeled variants of human carbonic anhydrase II and GroEL: evidence for increased flexibility of the hydrophobic core by the interaction, Biochemistry 38 (1999) 432–441.
[7] M. Lindgren, M. Svensson, P.O. Freskgard, U. Carlsson, B.H. Jonsson, L.-G. Mårtensson, P. Jonasson, Probing local mobility in carbonic-anhydrase-EPR of spin-labeled SH-groups introduced by site directed mutagenesis, J. Chem. Soc. Perkin. Trans. 2 (1993) 2003–2007.
[8] M. Lindgren, M. Svensson, P.O. Freskgard, U. Carlsson, P. Jonasson, L.-G. Mårtensson, B.H. Jonsson, Characterization of a folding intermediate of human carbonic-anhydrase-II-probing local mobility by electron paramagnetic resonance, Biophys. J. 69 (1995) 202–213.
[9] M. Lindgren, G.R. Eaton, S.S. Eaton, B.H. Jonsson, P. Hammarström, M. Svensson, U. Carlsson, Electron spin echo decay as a probe of aminoxyl environment in spin-labeled mutants of human carbonic anhydrase II, J. Chem. Soc. Perkin Trans. 2 (1997) 2549–2554.
[10] A. Zecevic, G.R. Eaton, S.S. Eaton, M. Lindgren, Dephasing of electron spin echoes for nitroxyl radicals in glassy solvents by non-methyl and methyl protons, Mol. Phys. 95 (1998) 1255–1263.
[11] L.-G. Mårtensson, B.-H. Jonsson, P.O. Freskgård, A. Kihlgren, M. Svensson, U. Carlsson, Characterization of folding intermediates of human carbonic anhydrase II. Probing substructure by chemical labeling of SH-groups introduced by site-directed mutagenesis, Biochemistry 32 (1993) 224–231.
[12] W. Blumberg, W. Mims, D. Zuckerman, Electron Spin Echo Envelope Spectrometry, Rev. Sci. Instrum. 4 (1973) 546–666.
[13] S. Dikanov, Y.D. Tsvetkov, Electron Spin Echo Envelope Modulation (ESEEM) Spectroscopy, CRC Press, Boca Raton, FL, 1992.
[14] R. Erickson, Simulation of ENDOR spectra of radicals with anisotropic hyperfine and nuclear quadrupolar interactions in disordered solids, Chem. Phys. 202 (1996) 263–275.
[15] A. Lund, R. Erickson, EPR and ENDOR simulations for disordered systems: The balance between efficiency and accuracy, Acta Chem. Scan. 52 (1998) 261–274.
[16] R.M. Kadam, Y. Itagaki, N.P. Benetis, A. Lund, R. Erickson, M. Huber, W. Hilczer, An EPR, ENDOR and ESEEM study of the benzene radical cation in CFCl3 matrix: isotopic substitution effects on structure and dynamics, Phys. Chem. Chem. Phys. 1 (1999) 4967–4974.
[17] M.L. Connolly, Solvent-Accessible Surfaces of Proteins and Nucleic Acids, Science 221 (1983) 709–713.
[18] F.M. Richards, B. Lee, The Interpretation of Protein Structures: Estimation of Static Accessibility, J. Mol. Biol. 55 (1971) 379–400.
[19] P. Hammarström, M. Persson, P.O. Freskgard, L.-G. Mårtensson, D. Andersson, B.-H. Jonsson, U. Carlsson, Structural Mapping of the Aggregation Nucleation Site in a Molten Globule Intermediate, J. Biol. Chem. 274 (1999) 32897–32903.
[20] J.A. Weil, J.R. Bolton, J.E. Wertz, Electron Paramagnetic Resonance, John Wiley & Sons, New York, 1994.
[21] A.D. Milov, K.M. Salikhov, Y.D. Tsvetkov, Phase relaxation of hydrogen atoms stabilized in an amorphous matrix, Sov. Phys. Solid State 15 (1973) 802–806.
[22] S. Dikanov, A. Astashkin, Y.D. Tsvetkov, Complexes of a Stable Nitoxyl Radical with Hydroxyl-containing Molecules in Frozen Solution, J. Struct. Chem. 23 (1982) 333–345.
[23] G. Martini, S. Ristori, M. Romanelli, L. Kevan, Adsorption of Nitroxide D_2O Solutions on X-Zeolite and Y-Zeolite Studied by Electron-Spin-Resonance and Electron-Spin Echo Spectroscopies, J. Phys. Chem. 94 (1990) 7607–7611.
[24] R. Langen, K.J. Oh, D. Cascio, W.L. Hubbell, Crystal structures of spin labeled T4 lysozyme mutants: Implications for the interpretation of EPR spectra in terms of structure, Biochemistry 39 (2000) 8396–8405.
[25] P. Loop, Distance Measurements in Biological Systems by EPR, in: L.J. Berliner, S.S. Eaton, G.R. Eaton (Eds.), Biological Magnetic Resonance, 2000, p. 19.